

# Beyond Linearization: Attributed Table Graphs for Table Reasoning

Yuxiang Wang<sup>1</sup>, Junhao Gan<sup>1</sup>, Shengxiang Gao<sup>1</sup>, Shenghao Ye<sup>2</sup>, Zhengyi Yang<sup>3</sup>, Jianzhong Qi<sup>1</sup>

<sup>1</sup>The University of Melbourne <sup>3</sup>The University of New South Wales

<sup>2</sup>The University of Science and Technology of China

{yuxiang.wang8, shengxiang.gao1}@student.unimelb.edu.au

{junhao.gan, jianzhong.qi}@unimelb.edu.au

ssh0321y@mail.ustc.edu.cn, yangzhengyi188@hotmail.com

## Abstract

Table reasoning, a task to answer questions by reasoning over data presented in tables, is an important topic due to the prevalence of knowledge stored in tabular formats. Recent solutions use Large Language Models (LLMs), exploiting the semantic understanding and reasoning capabilities of LLMs. A common paradigm of such solutions linearizes tables to form plain texts that are served as input to LLMs. This paradigm has critical issues. It loses table structures, lacks explicit reasoning paths for result explainability, and is subject to the “lost-in-the-middle” issue. To address these issues, we propose Table Graph Reasoner (TABGR), a training-free model that represents tables as an Attributed Table Graph (ATG). The ATG explicitly preserves row-column-cell structures while enabling graph-based reasoning for explainability. We further propose a Question-Guided Personalized PageRank (QG-PPR) mechanism to rerank tabular data and mitigate the lost-in-the-middle issue. Extensive experiments on two commonly used benchmarks show that TABGR consistently outperforms state-of-the-art models by up to 9.7% in accuracy. Our code will be made publicly available upon publication.

## 1 Introduction

Table reasoning aims to answer questions by reasoning over data presented in tables. Its importance comes from the prevalence of knowledge stored in tabular formats (Yu et al., 2025).

Recent studies leverage the semantic understanding and reasoning capabilities of Large Language Models (LLMs) for table reasoning. They typically follow two paradigms: (i) *decomposition-based reasoning*, which generates executable code or conduct iterative symbolic operations to decompose tables, and then reasons over the decomposed subtables (Cheng et al., 2023; Ye et al., 2023; Wang et al., 2024, 2025; Yu et al., 2025; Zhang et al., 2025a), and (ii) *full-table reasoning*, which applies

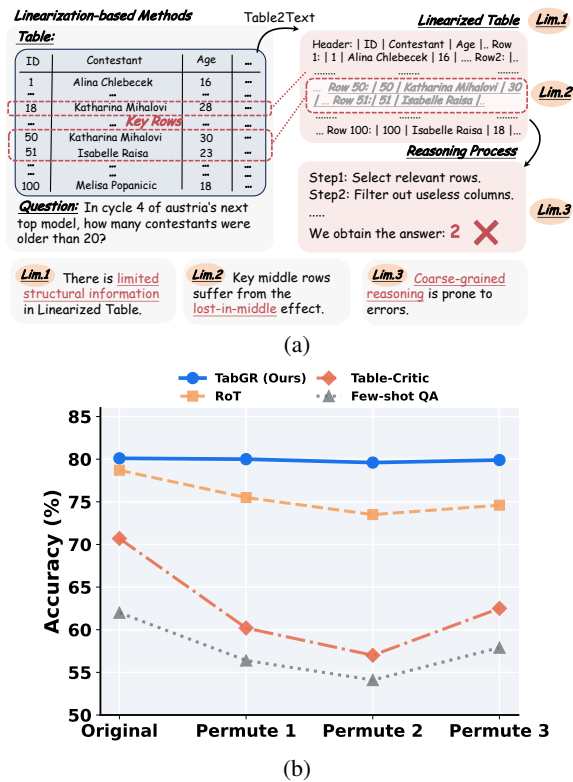


Figure 1: Motivating example. (a) Limitations of linearization-based methods. (b) Performance of different methods on WikiTableQuestions (Pasupat and Liang, 2015) under random table permutations.

LLMs to reason over full tables directly (Zheng et al., 2023; Liu et al., 2024b; Zhang et al., 2025b). Both paradigms linearize tables when feeding them into LLMs (Yin et al., 2020), treating tables as flat sequences (e.g., Markdown).

While table linearization is simple and has shown to be effective with existing solutions, we observe a few inherent limitations with such a table representation strategy, as illustrated by Figure 1.

**(1) Loss of structure information:** Linearizing tables easily loses their structure information, as LLMs tend to treat them as plain serialized text (see a case study in Appendix H), even though one may

add special tokens (e.g., ‘`s and newlines, cf. Figure 1a) to indicate columns and rows. A few existing methods preserve structure information through model architectural adaption and additional training (Yin et al., 2020; Su et al., 2024), which often requires substantial computational resources and extensive training process.

**(2) Sensitivity to answer positions:** Linearizing tables into a long sequence is vulnerable to the positions of the answers of the table reasoning tasks. LLMs are known to subject to the “lost-in-the-middle” problem (Liu et al., 2024a), i.e., they tend to miss information given in the middle of a long input. As shown in Figure 1b, we run two state-of-the-art (SOTA) methods, Table-Critic (Yu et al., 2025) and RoT (Zhang et al., 2025b), and a simple few-shot LLM prompting method on three random permutations of the table rows and columns of the WikiTableQuestions dataset (Pasupat and Liang, 2015). The table reasoning accuracy fluctuates with each permutation.

**(3) Lack of fine-grained reasoning:** Linearizing tables often constrains LLMs to plain-text reasoning, which lacks explicit structural grounding. As existing methods typically perform reasoning (e.g., Chain-of-Thought (Zheng et al., 2023)) over serialized texts, the resulting reasoning process is often coarse-grained, operating at the level of unstructured text spans rather than individual row-column-cell relations.

To address these limitations, we propose Table Graph Reasoner (TABGR), a novel table reasoning method that introduces an Attributed Table Graph (ATG) for table representation. In the ATG, rows and cells of a table is represented as the graph nodes, while the graph edges encode the column relations. This representation allows LLMs to access row-column-cell relations as graph triples.

Based on the ATG, we proposes a Question-Guided Personalized PageRank (QG-PPR) (Jeh and Widom, 2003; Brin and Page, 2012) mechanism to assign question- and structure-aware salience scores to each graph triple by inducing a propagation matrix, and we rerank triples according to their importance. This ensures that crucial information is surfaced to the LLM regardless of its original position in the table.

Besides, graph-based table reasoning allows LLMs to reason over explicit structural relations by identifying salient subgraphs, tracing reasoning paths, and revealing which row-column-cell connections support the final prediction, thereby

enabling more fine-grained reasoning and improving result explainability.

Our contributions are summarized as follows:

(1) We propose TABGR, a training-free table reasoning model that represents tables as an Attributed Table Graph, explicitly preserving the row-column-cell structure to achieve more effective reasoning.

(2) We introduce a Question-Guided Personalized PageRank mechanism that assigns salience scores to table (i.e., graph) triples, enabling question- and structure-aware triple reranking and hence improving robustness to answer position in tables (a.k.a. the “lost-in-the-middle” issue).

(3) We transform table reasoning into graph-based reasoning, enabling LLMs to produce fine-grained and structurally aligned reasoning paths that are easy to trace over the tables, thereby improving result explainability.

(4) Extensive experiments on Table Question Answering (TableQA) and Table Fact Verification (TableFV) benchmarks demonstrate that TABGR not only consistently outperforms SOTA methods in accuracy but also exhibits stronger robustness to permutations of table contents.

## 2 Related Work

Table reasoning requires models to comprehend both the content and structural information of tables, to support tasks such as TableQA and TableFV. Existing methods differ primarily in how they represent tables and reason over the represented format.

**Linearization-based Table Reasoning** Most existing methods for TableQA and TableFV follow a “linearize-then-reason” paradigm, converting tables into lineaized sequences (e.g., in Markdown format) before feeding them into LLMs. The methods can be further categorized into two groups.

Decomposition-based reasoning methods generate executable code or use iterative symbolic operations to decompose tables and/or questions. For example, Dater (Ye et al., 2023) decomposes tables and questions through LLM-generated programs. Binder (Cheng et al., 2023) uses LLMs to analyze full tables to generate programs that compute the answers, and re-invokes LLMs iteratively to refine the programs before execution. Chain-of-Table (Wang et al., 2024) employs step-wise reasoning, where an LLM iteratively applies pre-defined symbolic operations to derive a sub-table at each step. Table-Critic (Yu et al., 2025) further

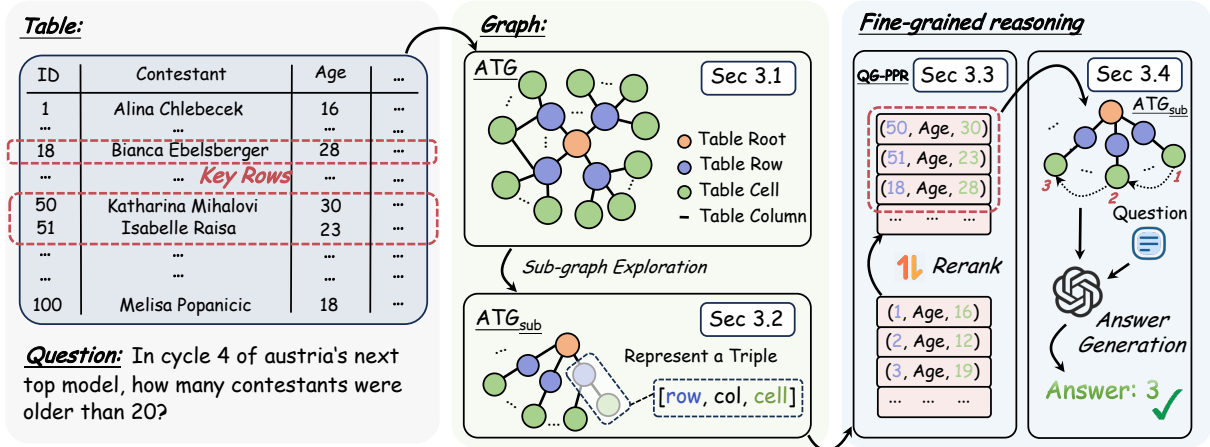


Figure 2: Overview of TABGR, a graph-based framework for table reasoning. The input table is first transformed into an Attributed Table Graph (ATG), which supports Question-Guided Personalized PageRank (QG-PPR) for estimating the salience of table triples and reranking evidence. The reranked evidence then guides an LLM to perform reasoning over the ATG, producing an explicit and fine-grained reasoning path.

enhances this pipeline by introducing intermediate critiques to refine each reasoning step.

Full-table reasoning methods utilize LLMs to reason over full tables. For example, TaCo (Zheng et al., 2023) performs Chain-of-Thought (CoT) (Wei et al., 2022) reasoning directly over fully linearized tables. RoT (Zhang et al., 2025b) improves CoT prompting by performing row-wise traversal reasoning using fully linearized tables.

Linearization-based input table representations are simply and intuitive. However, they break the row-column-cell structure of tabular data and form long input contexts, to which LLMs are vulnerable, i.e., LLMs may struggle to find answers hidden in the middle of a long input (a.k.a. the lost-in-the-middle issue (Liu et al., 2024a)).

**Graph Modeling for Tabular Tasks** Graph structures have been explored to capture dependencies in tabular data. For *table retrieval*, TRAG (Zou et al., 2025) employs a hypergraph to identify task-relevant tables under multi-table settings. For *multi-modal linking*, ODYSSEY (Agarwal et al., 2025) utilizes hybrid graphs to link tabular cells with external unstructured text. These methods still rely on *linearized tables* at inference time. GraphOTTER (Li et al., 2025) targets *complex table layout understanding* by transforming irregular tables into undirected graphs and performing predefined reasoning actions to traverse the graphs. Its graph representation focuses on local connections between cells by leveraging cell values together with their positional indices in the table as input to LLMs, which lacks global row-column-

cell structural awareness. The use of predefined reasoning actions may reduce flexibility and limit generalizability to table reasoning tasks beyond complex layout scenarios.

Different from these methods, TABGR represents tables as an ATG, which explicitly maintains row–column–cell connections and enables a QG-PPR mechanism. By deriving salience scores from the ATG rather than plain-text, TABGR can prioritize critical triples regardless of their original positions, thereby mitigating the lost-in-the-middle issues. Meanwhile, TABGR creates reasoning paths aligned with table topology, leading to enhanced result explainability.

### 3 TABGR

We consider an input table  $\mathcal{T}$  and an input question  $\mathcal{Q}$  (in plain-text) that we aim to answer through reasoning over  $\mathcal{T}$ .

As Figure 2 shows, our Table Graph Reasoner (TABGR) first transforms  $\mathcal{T}$  into an Attributed Table Graph (ATG, Section 3.1). The ATG explicitly encodes the row-column-cell structure of  $\mathcal{T}$  and serves two purposes: (1) It enables LLMs to perform graph-based table decomposition (Section 3.2), allowing TABGR to iteratively zoom in to the question-relevant elements of  $\mathcal{T}$ . (2) It induces a weighted propagation matrix for a Question-Guided Personalized PageRank (QG-PPR) mechanism (Section 3.3). By deriving salience scores from the ATG, TABGR reranks graph triples to prioritize the question-critical ones, hence mitigating the "lost-in-the-middle" issue. The reranked

triples are fed into an LLM for final answer generation (Section 3.4). This processing pipeline is summarized as Algorithm 1 in Appendix B.

### 3.1 Attributed Table Graph

We represent a table  $\mathcal{T}$  as an attributed table graph  $\mathcal{G} = (\mathcal{V}, \mathcal{E})$ , where the node set  $\mathcal{V}$  contains three types of nodes: (1) cell value nodes  $c_j^{(k)}$ , each corresponding to the  $k$ -th unique value in column  $col_j$ ; (2) row anchor nodes  $r_i$ , each representing a table row; and (3) a root node representing the entire table and connected to all row anchor nodes. Each cell value node  $c_j^{(k)}$  is connected to all row anchor nodes whose rows contain this value in column  $col_j$ , and each edge  $(r_i, c_j^{(k)}) \in \mathcal{E}$  is annotated with the column header  $h_j$ . Importantly, identical values appearing in different columns are treated as distinct nodes and are not merged across columns.

Accordingly, table  $\mathcal{T}$  can be viewed as a collection of structured triples defined at the cell level:

$$\langle r_i, h_j, c_{i,j} \rangle, \quad i \in [1, R], j \in [1, C], \quad (1)$$

assuming  $R$  rows and  $C$  columns in  $\mathcal{T}$ , and  $c_{i,j}$  denotes the value appearing at row  $r_i$ , column  $col_j$ . In the graph representation, all triples that share the same column  $col_j$  and value  $c_{i,j}$  are connected to the same cell value node  $c_j^{(k)}$ .

Constructing  $\mathcal{G}$  takes  $O(R \cdot C \cdot \log R)$  time, where  $R \cdot C$  means to go over each row and column of  $\mathcal{T}$ , and the  $\log R$  term is to check if a cell node corresponding to the value in a column of a row has been created already (for uniqueness). This process can be done offline if  $\mathcal{T}$  is given beforehand, where the resulting graph takes  $O(R \cdot C)$  space to store.

### 3.2 ATG-Based Table Decomposition

TABGR traverses  $\mathcal{G}$  to construct a grounded reasoning subgraph that is meant to contain task-relevant structural units (i.e., triples).

The traversal (i.e., reasoning) process starts by identifying *anchor triples*. These include (i) triples whose cell values  $c_{i,j}$  *exactly* match a sub-string of the input question  $Q$ , and (ii) triples whose edge attribute  $h_j$  is considered relevant to  $Q$  by an LLM.

We then iteratively expand the subgraph (i.e. extracted triples), using an LLM *judge* to determine if the current subgraph is sufficient to answer  $Q$ . If not, TABGR iteratively selects more columns (multiple columns are allowed for each step), and it adds triples matching the selected columns to the extracted subgraph. Otherwise, the traversal is

terminated, and the resulting subgraph, denoted by  $\mathcal{G}^*$ , is passed to the next step for triple reranking.

### 3.3 Question-Guided Personalized PageRank

Next, we present our QG-PPR mechanism to rerank triples in  $\mathcal{G}^*$ , such that the question-critical triples will surface at the top, to catch the attention of LLMs when they are fed into LLMs for reasoning and answer generation.

**Triple Salience Scores** We compute triple-level salience scores using QG-PPR, which is an adapted Personalized PageRank process, with the following iterative update:

$$\mathbf{s}^{(t+1)} = \alpha \mathbf{p}_0 + (1 - \alpha) \hat{A}^\top \mathbf{s}^{(t)}, \quad (2)$$

where  $\mathbf{s}^{(t)} \in \mathbb{R}^{n \times 1}$  ( $n$  is the number of triples in  $\mathcal{G}^*$ ) denotes the salience scores at iteration  $t$ ,  $\mathbf{p}_0$  is a *question-guided personalization vector* (detailed next),  $\hat{A}$  is the triple-level propagation matrix (detailed next), and  $\alpha \in (0, 1)$  is the teleport probability (Brin and Page, 2012).

We initialize  $\mathbf{s}^{(0)}$  with a uniform distribution and apply power iteration ( $K$  times) until convergence. In practice, we run 20 iterations, which is sufficient to obtain stable salience scores in our experiments.

**Personalization Vector** We define a personalization vector  $\mathbf{p}_0$ , which encodes the question-specific importance of each triple and serves as the restart distribution in Personalized PageRank.

Given a triple  $\langle r_i, h_j, c_{i,j} \rangle$ , we denote by  $p_0(i, j)$  the entry in  $\mathbf{p}_0$  associated with this triple. We initialize  $\mathbf{p}_0$  using question-aware signals from both exact string matching and an LLM-based semantic selector. We construct the key column name set  $\mathcal{H}_q$  and key cell value set  $\mathcal{C}_q$  by taking the union of (i) columns/cell values that exactly match a sub-string of  $Q$  and (ii) additional columns/cell values selected by the LLM based on semantic relevance. All matched candidates are deduplicated before scoring to avoid repeated counting.

Each triple receives an additive initial score:

$$p_0(i, j) = v_{\text{col}} \cdot \mathbb{I}(h_j \in \mathcal{H}_q) + v_{\text{val}} \cdot \mathbb{I}(c_{i,j} \in \mathcal{C}_q), \quad (3)$$

where  $\mathbb{I}(\cdot)$  denotes the indicator function. The entries of the personalization vector  $\mathbf{p}_0$  are then normalized such that  $\sum_{i,j} p_0(i, j) = 1$ , yielding a valid probability distribution over the triples. By default, we set  $v_{\text{col}} = 1.0$  and  $v_{\text{val}} = 2.0$ .

To further down-weights overly frequent cell values and emphasizes more informative values,

we incorporate an inverse document frequency (IDF) (Jones, 2004) term into the value-level contribution  $v_{\text{val}}$  by  $v_{\text{val}} \cdot \text{IDF}(c_{i,j})$ . Formally, for each cell value  $c_{i,j}$ , we define:

$$\text{IDF}(c_{i,j}) = \log \left( 1 + \frac{N}{1 + \text{df}(c_{i,j})} \right), \quad (4)$$

where  $N$  is the total number of rows in  $\mathcal{T}$  and  $\text{df}(c_{i,j})$  is the number of rows containing  $c_{i,j}$ .

**Propagation Matrix** To incorporate connectivity information between the triples, we induce a weighted triple-level propagation matrix  $\hat{A} \in \mathbb{R}^{n \times n}$ , projecting row- and column-level structural constraints onto transitions between triples. The matrix serves as the transition operator for propagating evidence probability from question-relevant triples to potential triples.

Two triples  $u$  and  $v$  are connected if they belong to the same row or share the same column header in  $\mathcal{G}^*$ . Their transition weight is defined as:

$$w_{u,v} = \begin{cases} \frac{w_{\text{row}}}{|\mathcal{C}(r_i)|}, & u, v \in \mathcal{C}(r_i), \\ \frac{w_{\text{col}}}{|\mathcal{C}(c_{j})|}, & u, v \in \mathcal{C}(c_{j}), \end{cases} \quad (5)$$

where  $\mathcal{C}(r_i)$  and  $\mathcal{C}(c_j)$  denote the set of triples from row  $r_i$  and column  $c_j$ , respectively, and  $|\cdot|$  represents set cardinality. Parameters  $w_{\text{row}}$  and  $w_{\text{col}}$  modulate the relative strength of information propagation along the row dimension and column dimension, which satisfies  $w_{\text{row}} + w_{\text{col}} = 1$ . This constraint guarantees that the sum of transition probabilities from any triple equals 1, preserving numerical stability during the subsequent QG-PPR iterations. By tuning these weights, we can flexibly prioritize row content or column content depending on the question type. Further, normalizing by  $|\mathcal{C}|$  ensures that the propagation intensity remains invariant to table size and permutation.

**Triple Reranking** We use the salience scores  $s$  derived from the QG-PPR process to rerank evidence both across rows and within each row. This reranking encourages question-critical triples to be placed at the start of the prompt to be fed into an LLM for reasoning and answer generation, regardless of their positions in the original table  $\mathcal{T}$ .

For each row  $r_i$ , we aggregate the salience scores of its associated triples to obtain a row-level importance score:

$$S(r_i) = \sum_j s_{i,j}, \quad (6)$$

where  $s_{i,j}$  denotes the salience score of triple  $\langle r_i, h_j, c_{i,j} \rangle$ . The rows are then ranked in descending order of  $S(r_i)$ .

Within each row, the corresponding triples are further ranked according to their individual salience scores  $s_{i,j}$  in descending order, yielding an intra-row ordering of cell-level evidence.

For *order-sensitive* questions, where the answer depends on the inherent order of the table (e.g., “who is the first listed player”), the original triple order is preserved. Such cases constitute less than 20% of our experimental datasets. For all other questions, the reranked triples are provided for the downstream reasoning. By prioritizing evidence based on graph-derived salience rather than original position in the table, TABGR effectively mitigates the “lost-in-the-middle” effect and achieves robust performance across different table permutations.

### 3.4 Answer Generation

The final stage of TABGR utilizes the reranked subgraph to generate both the final answer and explicit reasoning paths. Given question  $Q$  and the reranked subgraph  $\mathcal{G}_{\text{ranked}}^*$  (in the form of triples), we prompt an LLM to perform Chain-of-Thought (CoT) (Zheng et al., 2023) reasoning over  $\mathcal{G}_{\text{ranked}}^*$ .

The LLM is instructed to conduct reasoning by going through the graph triples. This process can be formulated as follows:

$$(P, T, Ans) = \text{LLM}(Q, \mathcal{G}_{\text{ranked}}^*), \quad (7)$$

where  $P = \{t_1, t_2, \dots, t_k\}$  represents the reasoning path consisting of the sequence of triples  $t_i \in \mathcal{G}_{\text{ranked}}^*$  that has been used to derive the answer;  $T$  denotes the CoT text, which provides the logical derivation grounded by path  $P$ , and  $Ans$  is the final generated answer.

By running the CoT process over the reranked graph triples rather than a linearized, plain-text table, TABGR effectively decouples reasoning from the table’s original sequence. This enables robustness against table permutations and provides a fine-grained reasoning process, as the LLM explicitly identifies the supporting reasoning path grounded by the triples from the structure of  $\mathcal{G}_{\text{ranked}}^*$ .

## 4 Experiments

### 4.1 Experimental Setup

**Datasets** We use two public table reasoning datasets, following a recent baseline, TableCritic (Yu et al., 2025): (i) WikiTableQuestions

Category	Method	LLaMA3.3-70B		Qwen2.5-72B		GPT-4o-mini		Average	
		WikiTQ	TabFact	WikiTQ	TabFact	WikiTQ	TabFact	WikiTQ	TabFact
Decomp.	Binder (Cheng et al., 2023)	52.2	80.5	57.0	82.2	54.8	83.3	54.7	82.0
	GraphOTTER (Li et al., 2025)	55.1	71.2	55.3	76.9	50.3	67.0	53.6	71.7
	Dater (Ye et al., 2023)	59.5	87.6	63.0	90.0	65.8	88.3	62.8	88.6
	Chain-of-Table (Wang et al., 2024)	62.1	89.9	68.3	89.7	67.5	88.9	66.0	89.5
	Table-Critic (Yu et al., 2025)	<u>70.1</u>	<u>91.5</u>	<b>77.2</b>	<u>92.6</u>	<u>73.9</u>	<u>91.1</u>	<u>73.7</u>	<u>91.7</u>
	<b>TABGR<sup>†</sup> (ours)</b>	<b>76.9</b>	<b>93.5</b>	<u>76.2</u>	<b>92.8</b>	<b>74.3</b>	<b>91.8</b>	<b>75.8</b>	<b>92.7</b>
Full-table	End-to-End QA	51.1	81.0	56.6	85.0	52.6	73.5	53.4	79.8
	Few-Shot QA	62.0	82.6	61.7	85.1	57.6	75.1	60.4	80.9
	Chain-of-Thought (Wei et al., 2022)	72.7	91.0	73.6	92.3	72.4	90.5	72.9	91.3
	RoT (Zhang et al., 2025b)	<u>78.7</u>	<u>92.6</u>	<u>77.3</u>	<u>93.6</u>	<u>74.2</u>	<u>92.0</u>	<u>76.7</u>	<u>92.7</u>
	<b>TABGR (ours)</b>	<b>80.1</b>	<b>94.4</b>	<b>79.2</b>	<b>94.0</b>	<b>77.1</b>	<b>92.3</b>	<b>78.8</b>	<b>93.6</b>
	Δ	↑ 1.8	↑ 1.9	↑ 2.5	↑ 0.4	↑ 3.9	↑ 0.3	↑ 2.7	↑ 1.0

Table 1: Overall table reasoning performance comparison. TABGR<sup>†</sup> represents our method with ATG-based table decomposition and TABGR represents our method with full-graph reasoning. **Bold** denotes the best performance and underline denotes the second-best. Δ (%) denotes the relative performance gain of TABGR and TABGR<sup>†</sup> comparing with the best baseline results.

Method	WikiTQ			TabFact	
	Small		Medium	Small	
	Small	Medium	Large	Small	Medium
# Questions	(3,625)	(638)	(81)	(1,942)	(82)
Table-Critic	72.1	60.8	<u>55.6</u>	91.7	87.8
RoT	<u>80.6</u>	<u>71.4</u>	54.3	<u>92.7</u>	<u>90.2</u>
TABGR <sup>†</sup>	78.6	67.4	<b>70.4</b>	93.6	92.7
<b>TABGR</b>	<b>82.1</b>	<b>72.3</b>	65.4	<b>94.5</b>	<b>93.9</b>
Δ	↑ 1.9	↑ 1.3	↑ 26.6	↑ 1.9	↑ 4.1

Table 2: Table reasoning performance comparison with the best baselines over tables in different size ranges: *small* (< 1k tokens), *medium* (1k–4k tokens), and *large* (> 4k tokens). TabFact has no *large* tables.

(denoted as WikiTQ) (Pasupat and Liang, 2015), a TableQA benchmark with 4,344 test samples from 421 tables. (ii) TabFact (Chen et al., 2020), a Table Fact Verification benchmark with 2,024 test samples from 298 tables. Further details of the two datasets can be found in Appendix C. To examine the generalizability of our method to more complex table structures, we further conduct experiments on HiTab (Cheng et al., 2022), a TableQA benchmark featuring hierarchical and complex tables. All results on HiTab are reported in Appendix G.

**Competitors** We compare our method TABGR (both w/ and w/o table decomposition, denoted as **TABGR<sup>†</sup>** and **TABGR**, respectively) with two categories of baseline methods:

(1) Decomposition-based reasoning: This category breaks down tables or questions into sub-

components before reasoning, including **Dater** (Ye et al., 2023), **Binder** (Cheng et al., 2023), **Chain-of-Table** (Wang et al., 2024), **Table-Critic** (Yu et al., 2025), and **GraphOTTER** (Li et al., 2025), which have been described in Section 2.

(2) Full-table reasoning: This category reasons over the full tables. **End-to-End QA** directly prompts an LLM with linearized full tables and questions. **Few-shot QA** adds examples (table, question, and the corresponding answer) to the LLM input. **Chain-of-Thought (COT)** (Wei et al., 2022) directly prompts an LLM to generate step-by-step reasoning over the linearized table. **RoT** (Zhang et al., 2025b) is also tested, which has been described in Section 2.

**Implementation Details** We run experiments with three LLM families of different sizes, including both open- and close-source ones: (i) GPT-4o-mini (Hurst et al., 2024), (ii) LLaMA3.3-70B-Instruct and LLaMA3.1-8B-Instruct (Dubey et al., 2024), and (iii) Qwen2.5-72B-Instruct (Yang et al., 2024). Unless specified otherwise, LLaMA3.3-70B-Instruct is used as the default backbone model across all methods tested in the same experiment.

For all baseline methods, we follow their original settings. For our methods, TABGR<sup>†</sup> uses ATG-based decomposition, while TABGR reasons over the full ATG. We set  $\alpha$  to 0.15 and 0.35 for the two modes, respectively (detailed hyper-parameter study is included in Appendix D). For all experiments, we use temperature 0.0, i.e., greedy decoding, to minimize randomness for result repro-

ducibility. The detailed prompts used for our methods are included in Appendix A.

**Evaluation Metrics** For WikiTQ, we use the official evaluator and report accuracy based on exact string matching (Pasupat and Liang, 2015). For TabFact, we report binary classification accuracy as the fact verification output is true or false.

All experiments are run with three NVIDIA A100 80 GB GPUs on a cloud GPU server.

## 4.2 Results

**Accuracy Results** Table 1 reports method performance across different LLM backbones on both datasets. We make the following observations:

(1) TABGR (with full graph reasoning) consistently outperforms all baseline methods across all three LLMs on both datasets. On average, TABGR achieves 78.8% accuracy on WikiTQ and 93.6% on TabFact, i.e., 2.7% and 1.0% improvements over with the over the strongest baseline, RoT, respectively. We run Paired t-test (Manfei et al., 2017) comparing TABGR with RoT, yielding p-val of 0.04 and 0.23 on the two datasets, respectively. This confirms that the results on WikiTQ is statistically significant, while the larger p-val on TabFact is due to the smaller test set size.

(2) While TABGR<sup>†</sup> (with ATG-based table decomposition) is not as accurate as TABGR, due to loss of information at the decomposition process, it outperforms all decomposition-based baselines, and is on-par with the strongest full-table reasoning baseline RoT. On average, TABGR<sup>†</sup> outperforms the state-of-the-art decomposition-based method, Table-Critic, by 2.8% and 1.1% on the two datasets, respectively. We notice that Table-Critic reported better result on WikiTQ with Qwen2.5-72B, as it takes advantage of the self-correction capabilities of the large LLM.

To further examine the usefulness of TABGR<sup>†</sup>, we break down the tables in the two datasets by size and report method performance over different table size categories in Table 2. We focus on TABGR, TABGR<sup>†</sup>, and the two best baselines Table-Critic and RoT (same below).

Overall, larger tables are more challenging, and the different methods report lower accuracy over larger tables. TABGR is the most accurate over small or medium tables, while TABGR<sup>†</sup> excels over large tables with more than 4,000 tokens, showing its effectiveness in identifying the most relevant subgraph for answer generation. The perfor-

Method	Shuffled WikiTQ		Shuffled TabFact	
	Row	Row & Col	Row	Row & Col
Table-Critic	↓ 14.1	↓ 18.7	↓ 9.7	↓ 14.0
RoT	↓ 4.1	↓ 6.2	↓ 0.9	↓ 1.1
TABGR <sup>†</sup>	↓ 0.9	↓ 1.3	↓ 0.5	↓ 0.7
<b>TABGR</b>	↓ 0.1	↓ 0.5	↓ 0.6	↓ 0.7

Table 3: Average relative accuracy changes (%), comparing with accuracy on the original datasets.

mance gap between our methods and the baseline methods is much larger on the large tables, emphasizing the "lost-in-the-middle" issue which is addressed by our QG-PPR triple reranking. In contrast, small tables yield the best performance for all methods due to low noise and short context. Notably, TABGR<sup>†</sup> performs even better on large tables than on medium-sized ones. This is because larger tables provide richer structural contexts, allowing our ATG-based decomposition and QG-PPR mechanism to effectively capture relevant information.

**Permutation Robustness** To evaluate the robustness of our methods against answer location in tables, we conduct a permutation analysis by shuffling the rows and columns of the tables (i.e. each row/column is swap with a randomly chosen row/column). We repeat the experiments twice with different random seeds and report the average performance drop comparing with that reported on the original tables. Note that there are questions in the datasets that rely on the original table structures, e.g., "who is the first listed player". There are a total of 747 and 409 such questions in WikiTQ and TabFact, respectively. We keep the tables unchanged for these questions.

As shown in Table 3, the two baseline models report substantial performance drops when the tables are shuffled. We conjecture that these methods may have been tuned for the original datasets.

Our TABGR methods exhibit superior robustness. There are only marginal drops in the accuracy, as our QG-PPR mechanism can help prioritize the question-relevant triples regardless of their initial positions in the tables. The slight drops can be explained by random effects of shuffling. Also, when multiple triples receive identical salience scores from the QG-PPR process, their relative order is determined by their order in the (shuffled) tables.

Category	Method	WikiTQ		TabFact	
		Input	Output	Input	Output
Decomposition	Table-Critic	31,192	875	30,681	1,008
	TABGR <sup>†</sup>	5,063	285	4,089	245
	Cost Ratio	0.16×	0.33×	0.13×	0.24×
Full-table	RoT	2,013	460	1,520	249
	TABGR	4,739	223	3,665	207
	Cost Ratio	2.35×	0.48×	2.41×	0.83×

Table 4: Token costs per question.

Method	WikiTQ	TabFact
Table-Critic	45.5	68.9
RoT	63.7	74.8
TABGR <sup>†</sup>	56.5	<b>75.5</b>
TABGR	<b>64.2</b>	75.2

Table 5: Accuracy comparison using LLaMA3.1-8B.

**Cost Efficiency** Table 4 reports the LLM calling costs in terms of the number of input/output tokens per question. TABGR<sup>†</sup> significantly reduces both the input and output tokens compared to the best decomposition-based baseline Table-Critic. For example, on WikiTQ, TABGR<sup>†</sup> consumes only 5,063 input tokens per question, achieving a 0.16× cost reduction comparing with that of Table-Critic. This reduction is primarily attributed to our ATG-based subgraph extraction, which effectively prunes irrelevant table content for the reasoning phase.

The decomposition-based methods incur higher costs than the full-table methods. This may look counter intuitive but is expected, as they require iterative LLM calls to decompose the tables, i.e., to trade efficiency for accuracy over large tables.

TABGR requires about 2.4× input tokens of that of the best full-table baseline RoT (e.g., 4,739 vs. 2,013 on WikiTQ). This increase is mainly due to the Personalization Vector construction (detailed in section 3.2), where the LLM is called to identify question-crucial information. Despite the higher input cost, TABGR reduces output token usage and thus output latency by avoiding repeated full-table reasoning as in RoT, since output latency is largely determined by the number of generated tokens.

We report ATG construction times in Appendix F, i.e., seconds for all tables in a dataset.

**Impact of LLM Size** To study the impact of the size of the backbone LLM, we use a smaller LLM, LLaMA3.1-8B, in addition to the LLMs used in Table 1. As shown in Table 5, the accuracy

Method	WikiTQ		TabFact	
	Acc.	Δ	Acc.	Δ
<b>TABGR<sup>†</sup></b>	<b>76.9</b>	-	<b>93.5</b>	-
w/o expansion	73.7	↓ 4.2	92.0	↓ 1.6
w/o QG-PPR	76.0	↓ 1.2	93.2	↓ 0.3
<b>TABGR</b>	<b>80.1</b>	-	<b>94.4</b>	-
w/o QG-PPR	79.5	↓ 0.8	93.8	↓ 0.6

Table 6: Ablation study results. Δ (%) indicates the relative performance drop when a module is removed.

drops for all methods comparing with those using LLaMA3.1-70B, which is expected. Our methods still outperform the best baselines in the respective categories, showing their robustness against LLM size. TABGR<sup>†</sup> is now slightly more accurate than TABGR on TabFact, because questions in TabFact mainly rely on localized evidence, making decomposition-based reasoning particular beneficial for the smaller LLM with limited information-filtering capability.

**Ablation Study** We study module effectiveness of our methods by introducing two variants: “w/o expansion” removes the iterative subgraph expansion process from our methods (i.e., using only the anchor triples), while “w/o QG-PPR” removes the QG-PPR triple reranking process (i.e., feeding all triples retrieved to an LLM without reranking).

The accuracy results in Table 6 demonstrate the essential role of our core modules in both decomposition and full-table scenarios.

**Other Results** We have also performed a parameter study, additional ablation studies, and a case study, as detailed in Appendices D to H.

## 5 Conclusion

We proposed TABGR, a training-free graph-based table reasoning method that represents tables as Attributed Table Graphs, which explicitly preserve row-column-cell structure and enable table-permutation robustness via a Question-Guided Personalized PageRank mechanism. Through reasoning over the attributed table graphs, we obtain fine-grained reasoning paths to enhance the result explainability. Extensive experiments show that our method outperforms state-of-the-art methods in accuracy, robustness to row and column ordering, and LLM token efficiency.

## 6 Limitations

While our experiments mainly focus on textual table reasoning, the proposed graph-based modeling and QG-PPR algorithm is not limited to text-only tables and could potentially be extended to multi-modal reasoning scenarios, where tabular data are combined with other modalities such as images. In addition, the datasets evaluated in this work are primarily English-based. Exploring the applicability of our method to tables in other languages is an important direction for future work.

## 7 Ethics Statement

All datasets and models used in this paper are publicly available, and their usage strictly adheres to the corresponding licenses and terms of use.

## References

Ankush Agarwal, Chaitanya Devaguptapu, and Ganesh S. 2025. Hybrid graphs for table-and-text based question answering using llms. In *NAACL*, pages 858–875.

Sergey Brin and Lawrence Page. 2012. Reprint of: The anatomy of a large-scale hypertextual web search engine. *Computer Networks*, 56(18):3825–3833.

Yihan Cao, Shuyi Chen, Ryan Liu, Zhiruo Wang, and Daniel Fried. 2023. Api-assisted code generation for question answering on varied table structures. In *EMNLP*, pages 14536–14548.

Wenhu Chen, Hongmin Wang, Jianshu Chen, Yunkai Zhang, Hong Wang, Shiyang Li, Xiyu Zhou, and William Yang Wang. 2020. TabFact: A large-scale dataset for table-based fact verification. In *ICLR*.

Zhoujun Cheng, Haoyu Dong, Zhiruo Wang, Ran Jia, Jiaqi Guo, Yan Gao, Shi Han, Jian-Guang Lou, and Dongmei Zhang. 2022. HiTab: A hierarchical table dataset for question answering and natural language generation. In *ACL*, pages 1094–1110.

Zhoujun Cheng, Tianbao Xie, Peng Shi, Chengzu Li, Rahul Nadkarni, Yushi Hu, Caiming Xiong, Dragomir Radev, Mari Ostendorf, Luke Zettlemoyer, and 1 others. 2023. Binding language models in symbolic languages. In *ICLR*.

Abhimanyu Dubey, Abhinav Jauhri, Abhinav Pandey, Abhishek Kadian, Ahmad Al-Dahle, Aiesha Letman, Akhil Mathur, Alan Schelten, Amy Yang, Angela Fan, and 1 others. 2024. The Llama 3 herd of models. *CoRR*, abs/2407.21783.

Aaron Hurst, Adam Lerer, Adam P. Goucher, Adam Perelman, Aditya Ramesh, Aidan Clark, AJ Ostrow, Akila Welihinda, Alan Hayes, Alec Radford, Aleksander Madry, Alex Baker-Whitcomb, Alex Beutel, and 1 others. 2024. GPT-4o system card. *CoRR*, abs/2410.21276.

Glen Jeh and Jennifer Widom. 2003. Scaling personalized web search. In *WWW*, pages 271–279.

Karen Spärck Jones. 2004. A statistical interpretation of term specificity and its application in retrieval. *Journal of Documentation*, 60(5):493–502.

Qianlong Li, Chen Huang, Shuai Li, Yuanxin Xiang, Deng Xiong, and Wenqiang Lei. 2025. GraphOTTER: Evolving llm-based graph reasoning for complex table question answering. In *COLING*, pages 5486–5506.

Nelson F. Liu, Kevin Lin, John Hewitt, Ashwin Paranjape, Michele Bevilacqua, Fabio Petroni, and Percy Liang. 2024a. Lost in the Middle: How language models use long contexts. *Transactions of the Association for Computational Linguistics*, 12:157–173.

Tianyang Liu, Fei Wang, and Muhao Chen. 2024b. Rethinking tabular data understanding with large language models. In *NAACL*, pages 450–482.

XU Manfei, Drew Fralick, Julia Z Zheng, Bokai Wang, M TU Xin, and FENG Changyong. 2017. The differences and similarities between two-sample t-test and paired t-test. *Shanghai archives of psychiatry*, 29(3):184.

Panupong Pasupat and Percy Liang. 2015. Compositional semantic parsing on semi-structured tables. In *ACL/IJCNLP*, pages 1470–1480.

Aofeng Su, Aowen Wang, Chao Ye, Chen Zhou, Ga Zhang, Gang Chen, Guangcheng Zhu, Haobo Wang, Haokai Xu, Hao Chen, Haoze Li, Haoxuan Lan, Jiaming Tian, Jing Yuan, Junbo Zhao, Junlin Zhou, Kaizhe Shou, Liangyu Zha, Lin Long, and 14 others. 2024. TableGPT2: A large multimodal model with tabular data integration. *CoRR*, abs/2411.02059.

Yuxiang Wang, Jianzhong Qi, and Junhao Gan. 2025. Accurate and regret-aware numerical problem solver for tabular question answering. In *AAAI*, pages 12775–12783.

Zilong Wang, Hao Zhang, Chun-Liang Li, Julian Martin Eisenschlos, Vincent Perot, Zifeng Wang, Lesly Miculicich, Yasuhisa Fujii, Jingbo Shang, Chen-Yu Lee, and 1 others. 2024. Chain-of-Table: Evolving tables in the reasoning chain for table understanding. In *ICLR*.

Jason Wei, Xuezhi Wang, Dale Schuurmans, Maarten Bosma, Brian Ichter, Fei Xia, Ed H. Chi, Quoc V. Le, and Denny Zhou. 2022. Chain-of-Thought prompting elicits reasoning in large language models. In *NeurIPS*, pages 24824–24837.

An Yang, Baosong Yang, Beichen Zhang, Binyuan Hui, Bo Zheng, Bowen Yu, Chengyuan Li, Dayiheng Liu, Fei Huang, Haoran Wei, Huan Lin, Jian

Yang, Jianhong Tu, Jianwei Zhang, Jianxin Yang, Jiaxi Yang, Jingren Zhou, Junyang Lin, Kai Dang, and 22 others. 2024. Qwen2.5 technical report. *CoRR*, abs/2412.15115.

Yunhu Ye, Binyuan Hui, Min Yang, Binhua Li, Fei Huang, and Yongbin Li. 2023. Large language models are versatile decomposers: Decompose evidence and questions for table-based reasoning. In *SIGIR*, pages 174–184.

Pengcheng Yin, Graham Neubig, Wen-tau Yih, and Sebastian Riedel. 2020. TaBERT: Pretraining for joint understanding of textual and tabular data. *arXiv preprint arXiv:2005.08314*.

Peiying Yu, Guoxin Chen, and Jingjing Wang. 2025. Table-Critic: A multi-agent framework for collaborative criticism and refinement in table reasoning. In *ACL*, pages 17432–17451.

Han Zhang, Yuheng Ma, and Hanfang Yang. 2025a. ALTER: augmentation for large-table-based reasoning. In *NAACL*, pages 179–198.

Xuanliang Zhang, Dingzirui Wang, Keyan Xu, Qingfu Zhu, and Wanxiang Che. 2025b. RoT: Enhancing table reasoning with iterative row-wise traversals. In *EMNLP*, pages 559–579.

Bowen Zhao, Changkai Ji, Yuejie Zhang, Wen He, Yingwen Wang, Qing Wang, Rui Feng, and Xiaobo Zhang. 2023. Large language models are complex table parsers. In *EMNLP*, pages 14786–14802.

Mingyu Zheng, Hao Yang, Wenbin Jiang, Zheng Lin, Yajuan Lyu, Qiaoqiao She, and Weiping Wang. 2023. Chain-of-Thought reasoning in tabular language models. In *EMNLP*, pages 11006–11019.

Jiaru Zou, Dongqi Fu, Sirui Chen, Xinrui He, Zihao Li, Yada Zhu, Jiawei Han, and Jingrui He. 2025. RAG over Tables: Hierarchical memory index, multi-stage retrieval, and benchmarking. *arXiv preprint arXiv:2504.01346*.

## A Prompts

### A.1 Prompts for Graph-Based Retrieval

The prompt used to select the key columns (i.e., edges) for the initial subgraph is as follows.

#### Initial column selection

You are a table analysis assistant.

Given:

- A table title
- A natural language question about the table
- A list of candidate columns from the table
- One sample row from the table

Task: Select the column names that contain the information necessary to answer the question. Only return the column names (split by commas), nothing else.

Here are some examples:

[Examples]

Title: {title}

Question: {question}

Candidate Columns: {candidate\_col}

Sample Row: {sample\_row}

Answer:

The prompt used to check if the subgraph fetched is sufficient for question answering is as follows.

#### Subgraph sufficiency check

You are given a TableQA question and multiple candidate reasoning paths.

Instructions:

- Use ONLY the candidate reasoning paths.
- Treat edges as UNDIRECTED: "(rowK; Col; X)" and "(X; Col; rowK)" both mean rowK have Col = X.
- Decide if the provided paths are sufficient to answer the question.
  - \* Sufficient: the given candidate paths can deterministically yield the answer.
  - \* Insufficient: necessary link(s) or value(s) are missing or ambiguous.
- If sufficient: Set Finished: True.
- If insufficient: Set Finished: False.
- Output exactly and only the following one section. Do NOT add any other text.

Here are some examples:

[Examples]

Title: {title}

Question: {question}

Candidate Reasoning Paths: {reasoning\_paths}

Finished:

The prompt used to select more edges (i.e., column headers) that are used to retrieve corresponding triples to expand the subgraph is as follows.

#### Additional edge selection

You are given a TableQA question, a set of (possibly incomplete) candidate reasoning paths, and a set of available relations from the same table graph.

Goal:

- Select the MINIMAL SUFFICIENT subset of relations from Available Relations which, when combined with the candidate reasoning paths, is enough to answer the question.

Rules:

- Use ONLY the relation(s) in provided available relations. Do NOT invent new facts.
- Minimality: choose the fewest relations ( $\geq 1$ ) among available relations that make the answer derivable.
- Tie-breaking: if multiple equally minimal subsets exist, preserve the original order in Available Relations (i.e., pick the earliest lines that work).

Output format (STRICT):

- Output exactly ONE line that starts with: SELECTED\_RELATIONS: followed by a Python list literal of strings, e.g. ['relation1', 'relation2'].
- Do NOT output anything else.

Here are some examples:

[Examples]

Title: {title}

Question: {question}

Candidate Reasoning Paths: {reasoning\_paths}

Available Relations: {available\_relations}

Sample Row: {sample\_row}

SELECTED\_RELATIONS:

### A.2 Prompts for Graph-Based Answer Generation

The prompt used to generate the final answers by both TABGR and TABGR<sup>†</sup> is as follows.

#### Answer generation

You are given a TableQA question and a list of candidate reasoning paths. Given a question, you should think it step by step and then answer the question. Also provide the final reasoning path encloses within <paths> ... </paths>.

Rules (strict):

- OUTPUT FORMAT: two sections:  
<think> <paths> ... </paths> ... </think>  
<answer> ... </answer>

Here are some examples:

[Examples]

YOUR TURN

Title: {title}

Question: {question}

Header: {header}

Table Content: {reasoning\_paths}

<think>

<paths>

---

**Algorithm 1:** Overall pipeline of TABGR<sup>†</sup>

---

**Input** :Table  $\mathcal{T}$ , question  $\mathcal{Q}$   
**Output** :Final answer  $Ans$ , Chain-of-Thought text  $T$ , and reasoning paths  $P$ .

```
1  $\mathcal{G} \leftarrow \text{GraphConstruction}(\mathcal{T})$                                  $\triangleright$  Represent  $\mathcal{T}$  as structured triples
2  $\hat{A} \leftarrow \text{InducePropagationMatrix}(\mathcal{G})$                           $\triangleright$  Triple-level transition operator
3  $\mathcal{G}^* \leftarrow \text{InitialExtraction}(\mathcal{Q}, \mathcal{G})$                     $\triangleright$  Exact match and relation selection
4  $suf \leftarrow \text{False}$ ,  $count \leftarrow 0$ 
5 while  $count < 3$  do
6    $suf \leftarrow \text{Judge}(\mathcal{Q}, \mathcal{G}^*)$                                       $\triangleright$  LLM-based subgraph sufficiency check
7   if  $suf = \text{True}$  then
8     break
9    $\mathcal{G}^* \leftarrow \mathcal{G}^* \cup \text{IterativeExpansion}(\mathcal{Q}, \mathcal{G})$             $\triangleright$  Select additional edges
10   $count \leftarrow count + 1$ 
11  $\mathbf{s} \leftarrow \text{QG-PPR}(\mathcal{Q}, \mathcal{G}^*, \hat{A})$                                  $\triangleright$  Salience estimation via Eq. (5)
12  $\mathcal{G}_{\text{ranked}}^* \leftarrow \text{Rerank}(\mathcal{G}^*, \mathbf{s})$                           $\triangleright$  Inter-row and intra-row reranking
13  $(P, T, Ans) \leftarrow \text{LLMReasoning}(\mathcal{Q}, \mathcal{G}_{\text{ranked}}^*)$             $\triangleright$  Generate grounded reasoning path and answer
14 return  $P, T$  and  $Ans$ .
```

---

## B Overall Method Pipeline

Algorithm 1 summarizes the processing pipeline of our TABGR<sup>†</sup> method. TABGR shares a similar pipeline, but without Lines 3 to 10. Its  $\mathcal{G}^*$  is just  $\mathcal{G}$ .

## C Dataset Details

Table 7 summarizes the two datasets used in the experiments.

Dataset	#Cols.	#Rows	#Toks.	#Toks.	#Toks.	#QA Pairs							
						/Tbl.	/Tbl.	/Tbl.	/Cell	/Ans.	Train	Val.	Test
TabFact	6.3	13.5	317.9	3.7	1.0	92,283	12,792	2,024					
WikiTQ	6.4	25.4	662.6	4.1	1.7	11,321	2,831	4,344					

Table 7: Dataset statistics. ‘Cols.’: Columns; ‘Toks.’: Tokens; ‘/Tbl.’: per table.

## D Hyper-parameter Study

### D.1 Impact of $w_{\text{row}}$ and $w_{\text{col}}$

We first tune the propagation weights  $w_{\text{row}}$  and  $w_{\text{col}}$  under the constraint  $w_{\text{row}} + w_{\text{col}} = 1$ . We evaluate a set of representative configurations as shown in Table 8, including column-oriented (larger  $w_{\text{row}}$ ), balanced, and row-oriented (larger  $w_{\text{col}}$ ) configurations. The best-performing configuration is selected based on validation performance and is used for result reported in the main experiments.

Across both WikiTQ and TabFact, TABGR consistently achieves its best performance with  $w_{\text{row}} =$

Method	$w_{\text{row}}$	$w_{\text{col}}$	WikiTQ		TabFact	
			Acc.	$\Delta$ (%)	Acc.	$\Delta$ (%)
TABGR <sup>†</sup>	0.1	0.9	75.8	↓ 1.4	92.4	↓ 1.2
	0.3	0.7	<b>76.9</b>	-	92.9	↓ 0.6
	0.5	0.5	76.4	↓ 0.7	93.2	↓ 0.3
	0.7	0.3	76.1	↓ 1.0	<b>93.5</b>	-
	0.9	0.1	74.2	↓ 3.5	92.1	↓ 1.5
TABGR	0.2	0.8	78.8	↓ 1.6	93.6	↓ 0.8
	0.4	0.6	79.4	↓ 0.9	94.0	↓ 0.4
	<b>0.6</b>	<b>0.4</b>	<b>80.1</b>	-	<b>94.4</b>	-
	0.8	0.2	78.5	↓ 2.0	93.3	↓ 1.2

Table 8: Impact of  $w_{\text{row}}$  and  $w_{\text{col}}$  ( $w_{\text{row}} + w_{\text{col}} = 1$ ).  $\Delta$  indicates the relative performance drop from the best result in each group.

0.6 and  $w_{\text{col}} = 0.4$ , indicating a stable preference for moderately stronger row-wise propagation. This suggests that TABGR often benefits from aggregating multiple attributes within the same row, while still preserving sufficient column-level interactions for cross-row comparison. In contrast, TABGR<sup>†</sup> exhibits more dataset-dependent sensitivity to the propagation weights. On WikiTQ, which typically requires multi-step reasoning involving cross-row filtering and comparison, a stronger column-wise propagation is preferred. On TabFact, which focuses on binary verification and often requires checking the consistency of multiple attributes within the same row, stronger row-wise propagation proves more effective.

From a reasoning perspective, these trends reflect how the two methods process information.

Method	$\alpha$	WikiTQ		TabFact	
		Acc.	$\Delta$ (%)	Acc.	$\Delta$ (%)
TABGR $^\dagger$	0.05	75.6	$\downarrow 1.7$	92.8	$\downarrow 0.7$
	<b>0.15</b>	<b>76.9</b>	-	<b>93.5</b>	-
	0.25	76.1	$\downarrow 1.0$	93.1	$\downarrow 0.4$
TABGR	0.25	79.2	$\downarrow 1.1$	93.9	$\downarrow 0.5$
	<b>0.35</b>	<b>80.1</b>	-	<b>94.4</b>	-
	0.45	79.5	$\downarrow 0.7$	94.0	$\downarrow 0.4$

Table 9: Impact of the teleport probability  $\alpha$ .  $\Delta$  (%) indicates the relative performance drop from the best result in each group.

TABGR performs global reasoning over the entire graph structure, allowing salience signals to propagate broadly and resulting in more stable performance across hyper-parameter settings. TABGR $^\dagger$ , by contrast, relies more on iterative reasoning over progressively constructed subgraphs, making its performance more sensitive to how relevance is propagated along row or column dimensions.

## D.2 Impact of $\alpha$

Next, we investigate the impact of the teleport probability  $\alpha$ , with results summarized in Table 9.

The optimal values of  $\alpha$  again vary for the two methods. TABGR $^\dagger$  achieves peak performance at  $\alpha = 0.15$ , whereas TABGR performs the best at  $\alpha = 0.35$ . This suggests that decomposition-based reasoning, which operates on subgraphs, benefits from a lower restart probability to allow for deeper structural propagation over the graphs. Conversely, reasoning over full tables requires a larger  $\alpha$  to maintain focus on question-relevant anchors, since it receives larger graphs.

## D.3 Impact of Number of Iterations in QG-PPR

Table 10 reports the impact of the power iteration count,  $K$ , used by QG-PPR. For both TABGR $^\dagger$  and TABGR, their accuracy improves slightly from  $K = 10$  to  $K = 20$  and remains unchanged at  $K = 30$ . Theoretically, the error of the power method for PPR decreases at a geometric rate of  $(1 - \alpha)^K$ . With our default teleport probability  $\alpha = 0.15$  for TABGR $^\dagger$  and  $\alpha = 0.35$  for TABGR, the residual error terms  $(0.85)^{20} \approx 0.038$  and  $(0.65)^{20} \approx 0.00018$  are sufficiently small to stabilize the relative ranking of the table triples.

Method	$K$	WikiTQ		TabFact	
		Acc.	$\Delta$ (%)	Acc.	$\Delta$ (%)
TABGR $^\dagger$	10	76.4	$\downarrow 0.7$	93.1	$\downarrow 0.4$
	<b>20</b>	<b>76.9</b>	-	<b>93.5</b>	-
	30	76.9	0.0	93.5	0.0
TABGR	10	79.8	$\downarrow 0.4$	94.2	$\downarrow 0.2$
	<b>20</b>	<b>80.1</b>	-	<b>94.4</b>	-
	30	80.1	0.0	94.4	0.0

Table 10: Impact of the number of iterations,  $K$ .

## D.4 Impact of the Initial Scoring Weights

We also evaluate the impact of the initial scoring weights  $v_{\text{col}}$  and  $v_{\text{cell}}$ , which affect the question-aware relevance distribution in the personalization vector  $\mathbf{p}_0$ .

As Table 11 shows, setting  $v_{\text{col}} = 1.0$  and  $v_{\text{cell}} = 2.0$  yields the best accuracy. This observation aligns with our intuition that column headers provide coarse structural guidance, while specific cell values play a more direct role in grounding evidence for reasoning. Incorporating the IDF term further adjusts  $v_{\text{cell}}$  by down-weighting frequent values, helping the methods emphasize more informative evidence. Overall, the relatively small performance variations across different configurations indicate that our graph-based propagation is robust to the choice of initial scoring weights.

$v_{\text{col}}$	$v_{\text{cell}}$	WikiTQ (Acc.)		TabFact (Acc.)	
		TABGR $^\dagger$	TABGR	TABGR $^\dagger$	TABGR
2.0	1.0	76.6	79.9	93.4	94.2
1.0	1.0	76.5	79.7	93.3	94.2
<b>1.0</b>	<b>2.0</b>	<b>76.9</b>	<b>80.1</b>	<b>93.5</b>	<b>94.4</b>

Table 11: Impact of the initial scores  $v_{\text{col}}$  and  $v_{\text{cell}}$ .

## E Additional Ablation Study

We conduct additional ablation study to further evaluate the effectiveness of QG-PPR.

In Table 12, we remove QG-PPR (“w/o QG-PPR”) and rerun our methods on the shuffled datasets as described earlier. Both TABGR and TABGR $^\dagger$  become more vulnerable to the shuffles, recording larger drops in accuracy, e.g., 5.9% vs. 0.5% for TABGR w/o QG-PPR and TABGR on WikiTQ with randomly shuffled rows and columns.

Table 13 reports accuracy results when QG-PPR is replaced by naive PageRank (“w/ PageRank”), which uses uniform initialization without a personalization vector, i.e., to propagates importance

Method	Shuffled WikiTQ		Shuffled TabFact	
	Row	Row & Col	Row	Row & Col
TABGR <sup>†</sup>	↓ 0.9	↓ 1.3	↓ 0.5	↓ 0.7
TABGR <sup>†</sup> w/o QG-PPR	↓ 6.0	↓ 7.1	↓ 1.0	↓ 1.2
TABGR	↓ 0.1	↓ 0.5	↓ 0.6	↓ 0.7
TABGR w/o QG-PPR	↓ 5.8	↓ 5.9	↓ 1.2	↓ 1.5

Table 12: Impact of QG-PPR on permutation robustness.

without explicitly modeling question relevance.

We further compare against a Few-Shot QA baseline with a row-based reranking strategy. Few-Shot QA relies on linearized table representations, and the row-based reranking ranks table rows according to LLM-predicted importance scores, with higher-ranked rows placed earlier in the LLM input. This setting allows us to examine whether simple LLM-based reranking is sufficient to improve reasoning performance under table linearization strategy.

The results show that both alternative reranking strategies result in accuracy drops. This indicates that reranking alone is insufficient to address the limitations of linearized table reasoning, and highlight the importance of explicitly modeling table structure, as enabled by QG-PPR’s graph-based representation and question-guided propagation.

Method	WikiTQ		TabFact	
	Acc.	Δ	Acc.	Δ
<b>Few-Shot QA</b>	<b>62.0</b>	-	<b>82.6</b>	-
w/ Row-based Reranking	58.9	↓ 5.0	74.3	↓ 10.0
<b>TABGR</b>	<b>80.1</b>	-	<b>94.4</b>	-
w/ PageRank	78.9	↓ 1.5	72.5	↓ 2.0

Table 13: Impact of QG-PPR on improving accuracy.

## F ATG Construction Time

Table 14 reports the ATG construction times. We see that it takes less then 5 seconds to construct the ATGs required for the 421 tables of the WikiTQ dataset, i.e., 0.010 s per table and it is even faster for TabFact, as the average table size is smaller in TabFact. Also, the maximum time (Max Time) taken for any table in the datasets is below 0.4 seconds, showing the high practicality of our method.

Dataset	# Questions	Total Time (s)	Avg. Time/Q (s)	Max Time (s)
WikiTQ	4,344	4.28	0.010	0.36
TabFact	2,024	0.73	0.002	0.15

Table 14: ATG construction times.

## G Experiments on HiTab

We further evaluate our method on HiTab to evaluate its generalizability. HiTab is characterized by its intricate hierarchical headers and nested structures, which pose a significant challenge.

To handle the hierarchical structures in HiTab, TABGR introduces two structural adaptations during triple construction to preserve structural and semantic context. First, we flatten multi-level column headers by recursively merging parent and child headers into a single semantic attribute path (e.g., Region-Worker Type-Metric), which is embedded into every triple in the column name  $h_j$ . Second, we adapt  $c_{i,j}$  by propagating row-level context by forward-filling merged cells in the left-most columns, ensuring that each triple captures the complete row hierarchy (e.g., Year-Industry).

We compare TABGR with recent methods, following their original implementations. In particular, TableParser (Zhao et al., 2023), GraphOTTER (Li et al., 2025), and TABGR are all evaluated using Qwen2-72B-Instruct as the backbone LLM, to ensure consistency with their reported settings.

As shown in Table 15, TABGR outperforms the strongest baseline GraphOTTER, which is also a graph-based reasoning method designed for complex table understanding. This result further demonstrates the flexibility of TABGR in handling more complex table structures.

Method	Accuracy
TableParser (Zhao et al., 2023)	44.6
GPT-3.5 (Zhao et al., 2023)	50.0
code-davinci-002 (Cao et al., 2023)	69.3
GraphOTTER (Li et al., 2025)	72.7
<b>TABGR (ours)</b>	<b>74.3</b>

Table 15: Accuracy results on HiTab.

## H Case Study

We conduct a case study comparing the output of our TABGR with those of two strong baselines: Table-Critic and RoT.

As shown in Figure 3, TABGR leverages the ATG structure to precisely identify empty cells, whereas RoT and Table-Critic suffer from structural misinterpretation and hallucination, leading to the incorrect inclusion of Row 1.

## Case Study

**Question:** During what time period was there no shirt sponsors?

**Gold Answer:** 1982–1985

**Table Content:**

Year	Kit Manufacturer	Shirt Sponsor	Back of Shirt Sponsor	Short Sponsor
1977–1978	[Empty]	National Express	[Empty]	[Empty]
1982–1985	Umbro	[Empty]	[Empty]	[Empty]
1985–1986	Umbro	Whitbread	[Empty]	[Empty]
1986–1988	Henson	Duraflex	[Empty]	[Empty]
1988–1989	[Empty]	Gulf Oil	[Empty]	[Empty]
...	...	...	...	...
2011–2013	Erreca	Mira Showers	Barr Stadia	Gloucestershire Echo

Model	Reasoning Process & Prediction
<b>TABGR (Ours)</b>	<p><b>Thought:</b> To find the time period when there was no shirt sponsor, we need to examine the "Shirt Sponsor" column in the table. The table lists various years and their corresponding shirt sponsors. We are looking for rows where the "Shirt Sponsor" is empty, indicating no sponsor. Upon reviewing the table, we find one row where the "Shirt Sponsor" is empty: (row2; Shirt Sponsor;) with the year range (row2; Year; 1982–1985). Therefore, the time period when there was no shirt sponsor is 1982–1985.</p> <p><b>Reasoning Path:</b> (row2; Shirt Sponsor;) → (row2; Year; 1982–1985)</p> <p><b>Prediction:</b> 1982–1985</p>
<b>Table-Critic</b>	<p><b>Thought:</b> To determine the time period with no shirt sponsor, we need to examine the "shirt sponsor" column in the original table. The rows with no shirt sponsor are: Row 1: 1977–1978 (no shirt sponsor); Row 2: 1982–1985 (no shirt sponsor). However, we also notice that there are other rows with no shirt sponsor: Row 6 is not one of them since it has gulf oil as the shirt sponsor, but row 1 and row 2 are. Given the information, the time period with no shirt sponsor is indeed 1977–1978 and 1982–1985. The Prediction Answer only mentions one of these time periods (1982–1985), but it does not account for the other time period (1977–1978). However, since 1982–1985 is indeed one of the correct time periods, the Prediction Answer is partially correct but incomplete.</p> <p><b>Analysis: Lost Structural Information and Model Confusion.</b> The critic misinterprets the table structure (identifying Row 1 as empty) and incorrectly penalizes the correct partial prediction, leading to an over-corrected redundant answer.</p> <p><b>Prediction:</b> 1977–1978, 1982–1985</p>
<b>RoT</b>	<p><b>Thought:</b> To answer the question, I need to figure out during which time period there was no shirt sponsor based on the given table. Let me look at the table again. The table has several columns: Year, Kit Manufacturer, Shirt Sponsor, Back of Shirt Sponsor, and Short Sponsor. My task is to find the time period when the "Shirt Sponsor" column is blank. Let me go through each row one by one. 1. 1977–1978: The "Shirt Sponsor" column is blank. That's one time period. 2. 1982–1985: The "Shirt Sponsor" column is also blank. That's another time period. 3. 1985–1986: The "Shirt Sponsor" column has a value, "Whitbread"... [omitted rows 4-17 for brevity, but similar logic]... So, the time periods when there was no shirt sponsor are 1977–1978 and 1982–1985.</p> <p><b>Analysis: Lost Structural Information.</b> The model incorrectly interprets Row 1 as blank, failing to ground "National Express" to its correct column due to the limitations of table linearization.</p> <p><b>Prediction:</b> 1977–1978, 1982–1985</p>

Figure 3: Case study comparing TABGR with strong baselines: Table-Critic and RoT.